Mechanical Properties and Fracture Behavior of Poly(vinylidene fluoride)-Polyhedral Oligomeric Silsesquioxane Nanocomposites by Nanotensile Testing

Fanlin Zeng[1,*], Yizhi Liu[1], Yi Sun[1]

[1] Department of Astronautic Science and Mechanics, Harbin Institute of Technology, Harbin, China
* Corresponding author: zengfanlin@hit.edu.cn

Abstract   The key static and dynamic mechanical properties and fracture behavior of nanocomposite films composed of a poly(vinylidene fluoride) (PVDF) matrix and different contents of polyhedral oligomeric silsesquioxane (FP-POSS) were researched by nano-tensile testing. The Young's modulus, storage modulus, loss modulus, loss tangent, yield strain, yield strength, tensile strength, fracture strength, fracture strain, fracture toughness and fracture deformations of all different nanocomposite systems were obtained. The influence of FP-POSS and its contents on the mechanical properties of PVDF was analyzed. Results showed that both the stiffness and toughness of PVDF were enhanced at some specific FP-POSS content and further additions of FP-POSS brought dramatic enhancements in toughness while associated with a decline in stiffness. Dynamical mechanical properties showed that FP-POSS increased the viscosity of PVDF. The mechanism of the effects of FP-POSS on PVDF was analyzed from the unique nano scale organic-inorganic molecular structure of FP-POSS and the micro structures of the nanocomposite films

Keywords   Poly(vinylidene difluoride), Polyhedral oligomeric silsesquioxanes, Nano-tensile, Mechanical properties, Fracture

1. Introduction

Poly(vinylidene difluoride) (PVDF) is a kind of semicrystalline polymer and widely used in smart structure sensors, actuators, and soft/thin transducers since it exhibits excellent piezoelectric and pyroelectric properties which derive from the two polar phases β and γ of PVDF [1, 2]. But unfortunately, neat PVDF can not completely meet the mechanical, thermal, and oxidation resistance property requirements of some harsh environments [3, 4]. Many efforts have been taken to improve the properties of PVDF. For example, incorporation of organic polymer or inorganic fillers into the PVDF matrix to produce composites has been extensively studied with the objective of further improving its properties [5-7]. However, few materials are miscible when melted with PVDF, and their improvement in one property is always accompanied by a deterioration in others. Over the past decade, Polyhedral oligomeric silsesquioxanes (POSS) have been widely known as a unique class of organic-inorganic hybrid materials which exhibits many superior thermomechanical properties in terms of wearability, thermal stability, oxidation resistance and high strength [8-10] because of the robust inorganic cage-like core structure with the Si-O atoms, while at the same time they perform very good bonding capability with polymeric base matrixes because of the alterable organic branches on the corners of the core. For a polymer matrix, it is widely accepted that inorganic fillers tend to improve in stiffness while organic ones in toughness. But as a kind of organic-inorganic hybrid compounds, how will fluorinated POSS influence the mechanical properties and fracture behaviors of PVDF needs to be researched. Our previous work has been proved that fluorinated POSS compounds and PVDF are fully miscible at any temperature and the miscibility is derived from the polar C-F bonds and the electrostatic interactions in the POSS and PVDF molecules [11]. The molecular dynamics simulation results show that the glass transition temperature of PVDF was significantly improved with $(3, 3, 3\text{- trifluoropropyl})_8Si_8O12$ (FP-POSS) [12] and the moduli of PVDF were improved and the improvement effect, in general, nearly decreased with the increase of the mass ratio of FP-POSS [13]. However, simulation results need to be verified from experiments. And in addition, some other key mechanical properties, especially the fracture properties can only be effectively obtained by this means.

As a standard mechanical test method, the tensile test has been widely used to determine some important mechanical properties such as Young's modulus, fracture toughness and yield stress of materials. But a traditional tensile test is not capable of a sample with nano scale size, where a very small tensile load and very precise measure equipments are needed. In recent years, the nano-tensile test has been developed and used to characterize the tensile behaviors of very small samples such as the nanotubes, silk, fibers and so on [14-16]. The nano-tensile test is also used to determine some dynamic mechanical properties by adding a very small harmonic force with specific frequency on the sample [17]. In this work, the PVDF/FP-POSS nanocomposites were firstly prepared by the solvent evaporation method. And then the nano-tensile testings were carried out. Although similar work has been performed and some valuable results have been given [18, 19], the focus of this work is on the tensile properties of PVDF/POSS at a relative high strain rate and the fracture behaviors were analyzed in detail from the experimental data and microscopy images.

2. Experimental

2.1. Materials and sample preparation

The detailed solvent evaporation method to prepare the neat PVDF and its FP-POSS nanocomposites can be found in Ref. [18, 19]. The mass ratios of FP-POSS added to the PVDF matrix were 0%, 3%, 5%, and 8%, and nanocomposites with different FP-POSS contents are denoted as PVDF-FPi% (i = 0, 3, 5 and 8), which has the morphology of film with the thicknesses around 70~110 μm. In addition, the films were white and translucent, with the exception of neat PVDF, which appeared to be transparent. With increased percentage of FP-POSS, the transparency of the films declined. The images of PVDF-FP$_i$% (i = 0, 3, 5 and 8) films are shown as figure 1. Samples for nano-tensile testing were cut from these films. The size of the samples is about ~100um×~10mm (shown as figure 2, but not exactly the same size in each test).
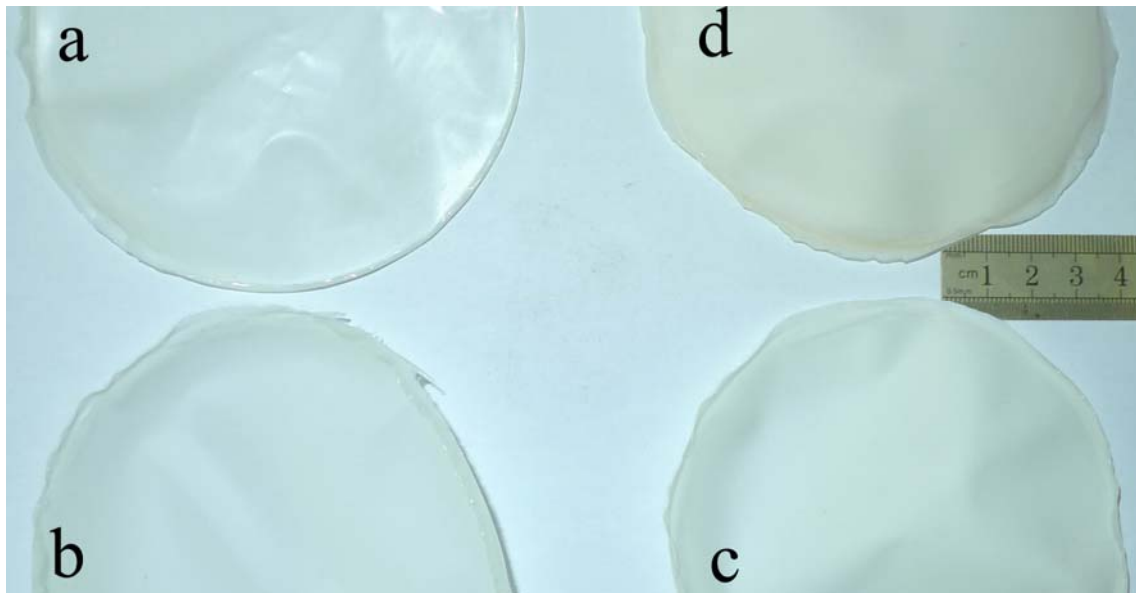

Fig. 1 Films of PVDF-FP$_i$% obtained by solution, i= (a) 0, (b) 3, (c) 5 and (d) 8.

2.3. Morphology and structure characterization

Optical microscopy was performed on the nanocomposite films to observe the fracture morphologies by using a VHX 600E digital microscope (Keyence Company) with a real-time depth composition, two/three-dimensional functions, and 20× to 5000× zoom. Scanning probe microscopy

(SPM) was performed using a SPM9500J2 microscope (Shimadzu Company) for images processing and profile analysis. The detailed results about the mciro structures and the crystallization of all the samples have been analyzed in Ref. [18].

2.3. Nano-tensile testing

A commercial nano-tensile testing system (Nano UTMTM Universal Testing System T150, Agilent Technologies, Inc.) with the method of UTM-Bionix Standard Toecomp CDA was used to conduct the tensile test in this paper. Detailed information and the image of the instrument were introduced in Ref. [18]. The samples were cut from PVDF-FP$_i$% films and seem like slender belts as shown in Fig. 2. The length and height of the belt like samples were measured by a caliper and screw micrometer, and the width was measured by the VHX 600E optical microscopy. Three individual samples have been prepared and tested in each category. The tensile strain rate was set as 1.0×10^{-2} s^{-1} here, which is ten times that of 1.0×10^{-3} s^{-1} in Ref. [18].
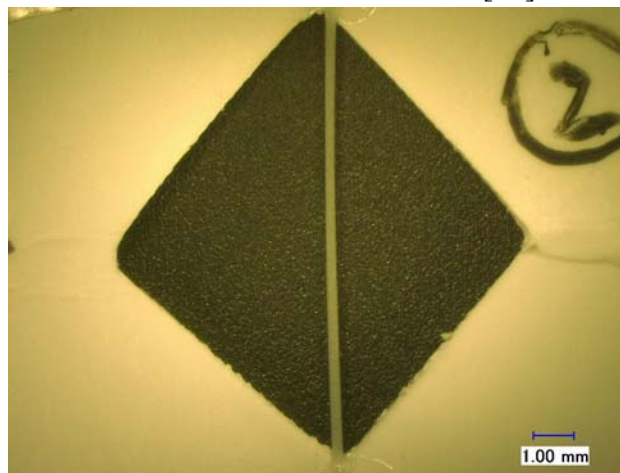

Fig.2. The image of the sample for the nano-tensile testing measured by optical microscopy.

3. Results and Discussion

3.1. Engineering stress-strain response

The engineering stress-strain responses for PVDF-FP$_i$% as obtained from the nano-tensile testing are shown in Fig. 3. The key points in these curves, such as the offset yield strain (0.2% offset), peak stress and break point, have been labeled as letters Y, P and B, respectively. The subscript numbers point out which sample these values belong to. The full stress-strain curves can be divided into three regions: (1) the elastic region (from the start point to Y), in which recoverable (elastic) deformation happens and the Hooke's law is satisfied between the stress and strain thus the Young's modulus can be computed. The stress at the offset yield strain point (σ_y) is called the tensile yield strength [20]; (2) the strain hardening region (Y→P), in which the stress is no longer proportional to strain and permanent nonrecoverable (plastic) deformation occurs. The stress at the maximum on the engineering stress–strain curve (point P) is defined as the tensile strength or ultimate strength [21]; (3) the unstable failure region (P→B), in which a small constriction or neck begins to form at some point, and fracture ultimately occurs at the neck. The fracture strength [20] corresponds to the stress at fracture and the area under the stress-strain curve up to the point of fracture is used to detect the fracture toughness, which is a measure of the ability of a material to absorb energy up to fracture and always used to delineate the brittleness or ductility of a material. All these key mechanical properties, for PVDF-FP$_i$% in the three regions are listed in table 1.
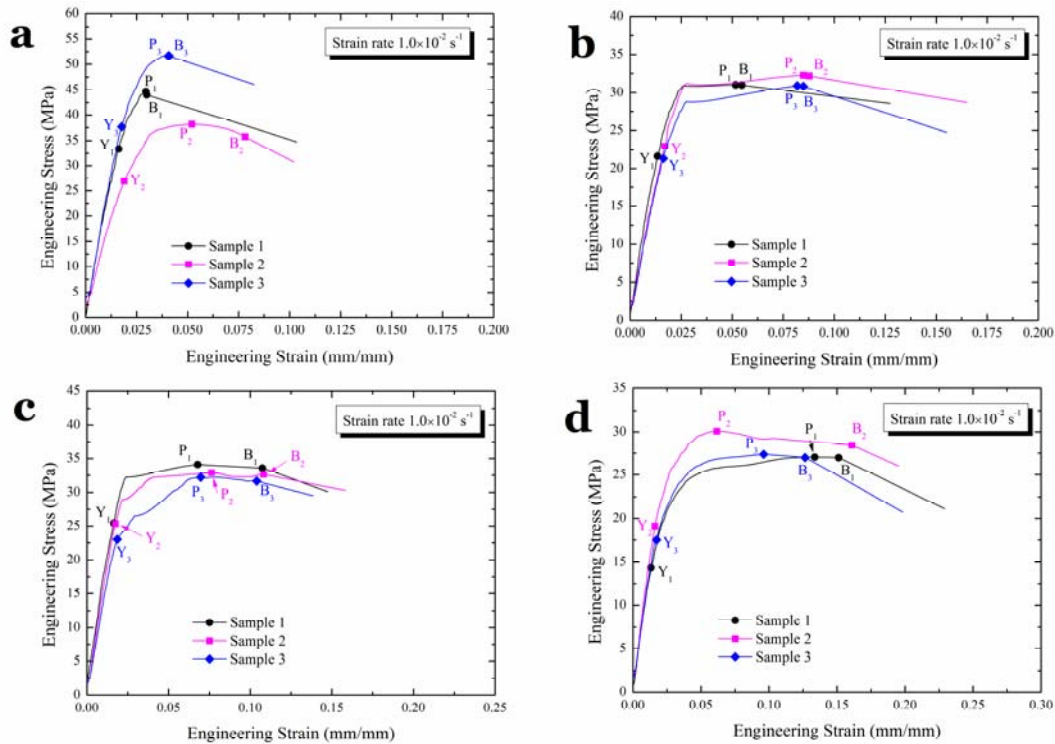
Fig. 3. Engineering stress-train response for PVDF-FP$_i$%, i= (a) 0, (b) 3, (c) 5 and (d) 8 at strain rate of 1.0×10^{-2} s^{-1}. The letters Y, P and B locate the positions of offset yield strain, peak stress and break point, respectively.

The Young's modulus of PVDF-FP$_{i\%}$ follows the orders PVDF-FP$_{0\%}$ > PVDF-FP$_{3\%}$ > PVDF-FP$_{5\%}$ > PVDF-FP$_{8\%}$. This means that the addition of FP-POSS reduced the modulus values of PVDF, which is quite different from the results in Ref. [13, 18]. This is probably resulted from two factors: (1) the much higher tensile strain rate, which is ten times that in Ref. [18]. A higher strain rate in tensile testing tends to achieve higher Young's modulus values. Thus nearly all the moduli of PVDF-FP$_{i\%}$ are greater than those obtained at the strain rate of 1.0×10^{-3} s^{-1} [18] except PVDF-FP$_{3\%}$; (2) the thinner film of PVDF-FP$_{0\%}$ (as shown in Fig.1, the film of PVDF-FP$_{0\%}$ is much thinner than the three other ones), which will bring the so called size effect during the tensile test and make the modulus value of PVDF-FP$_{0\%}$ become higher. But anyway, it is obvious that the elastic modulus of PVDF was weakened by further additions of FP-POSS at high strain rate. The values of yield strength (Y_S), tensile strength (T_S), and fracture strength (F_S) show a similar trend and indicate the FP-POSS contents have the similar effect on the strength of PVDF. The values of offset yield strain (ε_y) are almost the same for PVDF-FP$_{5\%}$ and PVDF-FP$_{0\%}$ and a little higher for PVDF-FP$_{3\%}$ and PVDF-FP$_{8\%}$, shows there is no obvious rule to describe the effect of FP-POSS on the elastic deformation range of PVDF at high strain rate.

The elongation at break (fracture strain) and fracture toughness values reveal an undoubtedly influence of FP-POSS on PVDF. The fracture strain and fracture toughness increase with the increasing content of FP-POSS. The value of εf increases from 4.9 % to 14.62 %, giving PVDF-FP$_8$% the toughness ~200 % higher than that of neat PVDF. Dramatic enhancements in fracture toughness can be observed when the FP-POSS content reaches to some extent. The content of 3 wt.% FP-POSS only brings a 26 % increase of the fracture toughness to PVDF (1.99 MPa vs. 1.58 MPa). However, when the content of FP-POSS reaches to 8 wt.%, the enhancement in fracture toughness will increase sharply to 130 % (3.63 MPa vs. 1.58 MPa). The similar mechanism to the toughness enhancements at high strain rate can be deduced from the microstructures of neat PVDF and its FP-POSS nanocomposites that have been detected [18]. The effect of FP-POSS in PVDF has

been proved to form bigger PVDF particles. FP-POSS act like the nucleating agents in PVDF mixtures and make more PVDF molecules be nucleated around them. Thus the particles are more separate and the domain size of the particles becomes larger with the increasing of the FP-POSS content. In contrast to the neat PVDF, more separate and less cross-linked particles in PVDF nanocomposites (especially in PVDF-FP$_5$% and PVDF-FP$_8$%) lead to a structure much more conductive to plastic flow under applied stress and result in a more efficient energy-dissipation, thereby reducing crack formation [22].

Table 1. The Young's modulus (E), offset yield strain (ε_y), yield strength (Y_S), tensile strength (T_S), fracture strength (F_S), fracture strain (ε_f) and fracture toughness (K_c) of PVDF-FP$_i$% (i = 0, 3, 5 and 8) as obtained from stress-strain responses and hardness values.

FP-POSS (wt.%)	E (GPa)	ε_y (%)	Y_S(MPa)	T_S (MPa)	F_S (MPa)	ε_f (%)	K_c (MPa)
0	2.17(0.46)	1.73(0.12)	32.14(6.21)	44.83(6.76)	44.18(7.75)	4.90(2.40)	1.58(0.80)
3	1.65(0.21)	1.53(0.21)	21.99(0.85)	31.41(0.74)	31.35(0.72)	7.58(1.83)	1.99(0.53)
5	1.64(0.19)	1.73(0.15)	24.59(1.36)	33.04(0.96)	32.61(0.97)	10.66(0.22)	3.05(0.24)
8	1.27(0.11)	1.56(0.21)	16.98(2.43)	28.17(1.67)	27.47(0.83)	14.62(1.78)	3.63(0.65)

Note: Values in parentheses indicate ($\pm$) standard deviations.

3.2. Dynamic mechanical properties

There is a sensitive spring installed in T150 which can provide a very small harmonic force with specific frequency on the sample thus the dynamic mechanical properties of PVDF-FP$_i$%, such as the storage modulus, loss modulus and loss tangent can also be obtained during the tensile procedure. To viscoelastic materials, the storage modulus measures the stored energy, representing the elastic portion; and the loss modulus illustrates the energy dissipated as heat, representing the viscous portion ; the loss tangent is defined as the ratio of viscous to elastic portion and would change with the storage and loss modulus. The value of loss tangent is important to measure the viscoelastic properties of a material. A value of 0 means that a material is fully elastic while a high value represents a material with high viscosity. Dynamic mechanical properties are helpful to understanding and confirming the energy-dissipation mechanism for PVDF-FP$_i$% as analyzed previously.

Table 2 lists the values of storage modulus (G'), loss modulus (G'') and loss tangent (tan δ) for PVDF-FP$_{i\%}$ (i = 0, 3, 5 and 8) obtained from the nano-tensile testing at the harmonic force of 4.5 mN and the frequency of 20 Hz. It can be observed that all the values of storage modulus are higher than the corresponding values of Young's modulus as obtained from the elastic portion of stress-strain responses (listed in table 1). This is not surprising since the storage modulus is averaged within the whole range of stress-strain responses, in which modulus with higher values is keeping after the yield strain due to a full elastic deformation. Loss modulus values for PVDF-FP$_{i\%}$ (i = 3, 5 and 8) show that the addition of FP-POSS obviously increases the viscosity of PVDF since they are much higher than that of the neat PVDF. Compared with the storage and loss modulus, loss tangent is more reliable to measure viscoelastic properties because it is the ratio of loss to storage modulus thus less influenced by the uncertain factors in measuring or some unpredictable defects in materials. The values of loss tangent in table 2 show an evidently viscosity increasing with the increasing content of FP-POSS. Compared with the loss tangent values obtained at the strain rate of 1.0×10^{-3} s^{-1} [18] (from 0.089 of neat PVDF to 0.113 of PVDF-FP$_{8\%}$), the values increase more obviously at the strain rate of 1.0×10^{-2} s^{-1} in this article (from 0.075 of neat PVDF to 0.151 of PVDF-FP$_{8\%}$), which shows the perspicuous effect of the strain rate on the viscosity of PVDF and its nanocomposites.

Table 2. The storage modulus (G'), loss modulus (G'') and loss tangent (tan δ) of PVDF-FP$_i$% (i = 0, 3, 5 and 8) as obtained from nano-tensile testing at a harmonic force of 4.5 mN and a frequency of 20 Hz.

FP-POSS (wt.%)	G' (GPa)	G'' (MPa)	tan δ
0	2.40(0.31)	169.2(78.5)	0.075(0.046)
3	1.86(0.17)	176.9(73.1)	0.097(0.065)
5	1.74(0.15)	186.0(74.9)	0.107(0.043)
8	1.43(0.18)	203.7(93.5)	0.151(0.099)

Note: Values in parentheses indicate ($\pm$) standard deviations.

3.3. Fracture appearance analysis

The fracture appearance of PVDF-FP$_i$% (i = 0, 3, 5 and 8) are shown in Fig.4. These images were obtained by VHX 600E with a real-time depth composition, three-dimensional functions at 500× or 1000× zoom. It can be found very clearly that the image of neat PVDF (Fig. 4 (a)) is quite different from the others. Compared with the three other ones, the fracture appearance of neat PVDF is more regular and the boundary is clear, shows only a small area near the fracture surface was obviously influenced during the fracture procedure. On the contrary, the fracture appearance of PVDF-FP$_i$% (i = 3, 5 and 8) (Fig. 4 (b), (c) and (d)) are irregular and the boundaries of the fracture surfaces are not obvious. These results have undoubtedly proved that the brittleness of neat PVDF is higher than its FP-POSS nanocomposites and the viscosity of PVDF will be increased by the addition of FP-POSS. Another important phenomenon is that the fracture regions of PVDF-FP$_i$% (i = 3, 5 and 8) are different. As shown in Fig. 4, the area of the fracture regions increases with the content of FP-POSS in PVDF, reveals that the brittleness drops and the viscosity rises when FP-POSS is mixed into PVDF. And more FP-POSS was mixed, more obvious this effect was displayed, which is in good agreement with the variation trend of the loss tangent values in section 3.2 and the fracture toughness values in section 3.1.
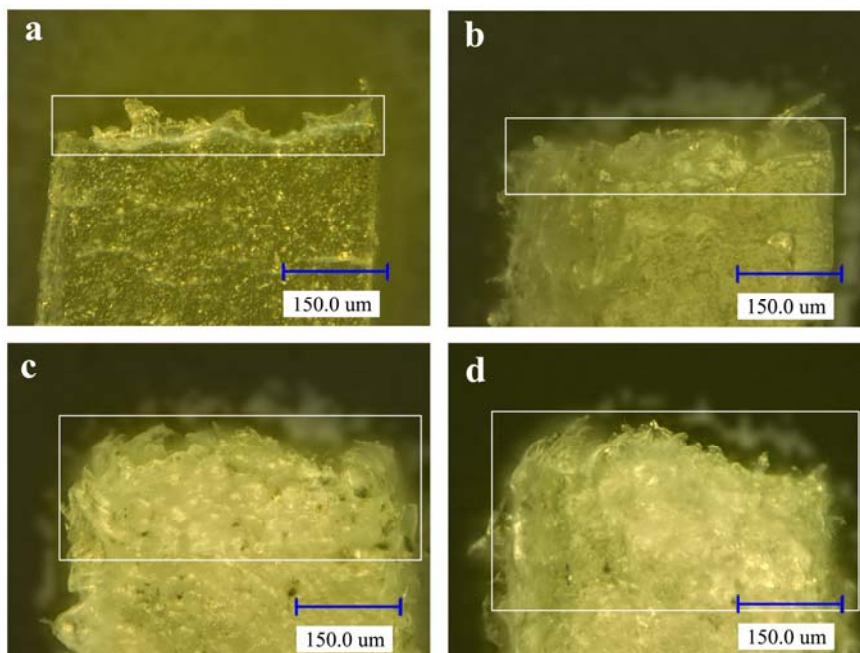

Fig. 4. Optical microscopy images of the fracture appearance for PVDF-FP$_i$% obtained by VHX 600E, i= (a) 0, (b) 3, (c) 5 and (d) 8. The square boxes locate the fracture regions.

4. Conclusions

PVDF/FP-POSS nanocompostites can be prepared by solvent evaporation method. Nano-tensile testing results at the strain rate of 1.0×10^{-2} s^{-1} showed the toughness of PVDF were enhanced by FP-POSS and further additions of FP-POSS brought surprisingly enhancements in toughness of the nanocomposites while associated with a decline in stiffness. Dynamical mechanical properties indicated the viscosity of the nanocomposites increased with the increasing FP-POSS contents in PVDF-FP$_{i\%}$. Fracture appearance analysis results showed that the fracture appearance of neat PVDF was regular and the boundary was clear, while PVDF-FP$_{i\%}$ (i = 3, 5 and 8) are irregular and not obvious. And the fracture regions increased with the content of FP-POSS in PVDF, which provided the visual evidence for the conclusions obtained from the data analysis. The great improvement effects on toughness and the increasing viscosity resulted from further additions of FP-POSS should be derived from the more separate and less cross-linked particles in the nanocomposites and the nano scale size of POSS compounds, which made the materials, are more easy to form plastic flow and more efficient on energy-dissipation.

References
[1] Seminara Lucia, Capurro Marco, Cirillo Paolo. Electromechanical characterization of piezoelectric PVDF polymer films for tactile sensors in robotics applications. Sensors and Actuators A-Physical, 169(1) (2011) 49–58.
[2] Kerur SB, Ghoshy A. Active vibration control of composite plate using AFC actuator and PVDF sensor. International Journal of Structural Stability and Dynamics, 11(2) (2011) 237–255.
[3] Dargaville TR, Celina M, Chaplya PM. Evaluation of Piezoelectric Poly(Vinylidene Fluoride) Polymers for Use in Space Environments. I. Temperature Limitations. Journal of Polymer Science Part B: Polymer Physics, 43 (2005) 1310–1320.
[4] Dargaville TR, Celina M, Martin JW, et al. Evaluation of Piezoelectric Pvdf Polymers for Use in Space Environments. II. Effects of Atomic Oxygen and Vacuum Uv Exposure. Journal of Polymer Science Part B: Polymer Physics, 43 (2005) 2503–2513.
[5] Xu HP, Dang ZM, Jiang MJ, Yao SH, Bai J. Enhanced dielectric properties and positive temperature coefficient effect in the binary polymer composites with surface modified carbon black. Journal of Materials Chemistry, 18 (2008) 229–234.
[6] Li YJ, Shimizu H. Conductive PVDF/PA6/CNTs nanocomposites fabricated by dual formation of cocontinuous and nanodispersion structures. Macromolecules, 41(14) (2008) 5339-5344.
[7] Malmonge LF, Langiano SD, Cordeiro JMM, et al. Thermal and Mechanical Properties of PVDF/PANI Blends. Materials Research-Ibero-American Journal of Materials, 13(4) (2011) 465–470.
[8] Fu BX, Gelfer MY, Hsiao BS, Phillips S, Viers B, Blanski R, P Ruth. Physical gelation in ethylene–propylene copolymer melts induced by polyhedral oligomeric silsesquioxane (POSS) molecules. Polymer, 44(5) (2003) 1499–1506.
[9] Deng J, Polidan JT, Hottle JR, Farmer-Creely CE, Viers BD, Esker A. Polyhedral Oligomeric Silsesquioxanes: A New Class of Amphiphiles at the Air/Water Interface. Journal of the American Chemical Society, 124(51) (2002) 15194.
[10] Fu BX, Hsiao BS, White H, Rafailovich M, Mather PT, Jeon HG, Phillips S, Lichtenhan J,

Schwab J. Nanoscale reinforcement of polyhedral oligomeric silsesquioxane (POSS) in polyurethane elastomer. Polymer International, 49(5) (2000) 437–440.

[11] Zeng FL, Sun Y, Zhou Y, Li QK. Molecular simulations of the miscibility in binary mixtures of PVDF and POSS compounds. Modelling and Simulation in Materials Science and Engineering, 17, (2009) 075002.

[12] Mabry JM, Vij A, Iacono ST, Viers BD. Fluorinated Polyhedral Oligomeric Silsesquioxanes (F-POSS). Angewandte Chemie International Edition, 47(22) (2008) 4137–4140.

[13] Zeng FL, Sun Y, Zhou Y, Li QK. A molecular dynamics simulation study to investigate the elastic properties of PVDF and POSS nanocomposites. Modelling and Simulation in Materials Science and Engineering, 19 (2011) 025005.

[14] Tan EPS, Ng SY, Lim CT. Tensile testing of a single ultrafine polymeric fiber. Biomaterials, 26 (2005) 1453–1456.

[15] Kiuchi M, Matsui S, Isono Y. Mechanical characteristics of FIB deposited carbon nanowires using an electrostatic actuated nano tensile testing device. Journal of Microelectromechanical Systems, 16(2) (2007) 191–201.

[16] Seydel T, Knoll W, Greving I, etal. Increased molecular mobility in humid silk fibers under tensile stress. Physical Review E, 83(1) (2011) 016104.

[17] Chang WY, Fang TH, Lin YC. Thermomechanical and optical characteristics of stretched polyvinylidene fluoride. Journal of Polymer Science Part B: Polymer Physics, 46(10) (2008) 949–958.

[18] Fanlin Zeng, Yizhi Liu, Yi Sun, Enlai Hu, Yu Zhou. Nanoindentation, Nanoscratch and Nanotensile Testing of Poly(vinylidene fluoride)-Polyhedral Oligomeric Silsesquioxane Nanocomposites. Journal of Polymer Science Part B: Polymer Physics, 50(23) (2012) 1597–1611.

[19] Liu Yizhi, Sun Yi, Zeng Fanlin, etal. Morphology, crystallization, thermal and mechanical properties of poly(vinylidene fluoride) films filled with different concentrations of polyhedral oligomeric silsesquioxane. Polymer Engineering & Science, DOI: 10.1002/pen.23398.

[20] William D, Callister Jr. Materials Science and Engineering An Introduction (7th ed). John Wiley & Sons, United States of America, 2006.

[21] Dowling N E. Mechanical Behavior of Materials (2nd ed). Prentice Hall PTR, Paramus, NJ, 1998.

[22] Shah D, Maiti P, Gunn E. Dramatic enhancements in toughness of polyvinylidene fluoride nanocomposites via nanoclay-directed crystal structure and morphology. Advanced Materials, 16(14) (2004) 1173–1177.